Volume 1 | Number 1 | Jan 2013 | Pages 1–100

ChemComm

Chemical Communications
www.rsc.org/chemcomm

ROYAL SOCIETY OF CHEMISTRY

ROYAL SOCIETY OF CHEMISTRY

www.rsc.org/chemcomm

Journal Name

COMMUNICATION

Cu(II)/Cu(0)@UiO-66-NH₂: base metal@MOFs as heterogeneous catalysts for olefin oxidation and reduction

Jian-Cheng Wang, Yu-Hong Hu, Gong-Jun Chen, and Yu-Bin Dong∗

Two copper-loaded MOF materials, namely Cu(II)@Ui-O-66-NH₂ (1) and Cu(0)@UiO-66-NH₂ (2), are reported. They can respectively serve as the highly efficient heterogeneous catalysts for olefin oxidation and hydrogenation under mild conditions. Complete styrene hydrogenation occurs at 15 min. under ambinet temperature with quantitative yield.

As a new type of heterogeneous catalytic materials, metal-loaded metal-organic frameworks (metal@MOFs) have been attracted more and more attention.[1] Although significant progress has recently been achieved in this very active field, the metal species used for fabrication of metal@MOFs are mainly focused on precious metals such as Pd, Pt, Au, Ru, Rh, Ir, Ag and so on.[2] In contrast, the earth-abundant metal (base metal) elements are relatively rarely used to design and synthesis of metal@MOFs catalysts.[3] On the other hand, new types of base metal-loaded MOF heterogeneous catalytic systems are imperative because of more and more serious sustainable and environmental issues.

With above issues in mind, we report here two new base metal@MOFs Cu(II)@UiO-66-NH₂ (**1**) and Cu(0)@UiO-66-NH₂ (**2**), which is generated from nano-sized UiO-66-NH₂ and Cu(OAc)₂ via the simple solution impregnation (for **1**), and the following metal ion reduction process (for **2**). The resulted Cu(II)/Cu(0)@UiO-66-NH₂ can be highly active heterogeneous catalysts for olefin oxidation (by **1**) and reduction (by **2**), respectively.

The combination of Cu(OAc)₂ and UiO-66-NH₂ nano-crystals in EtOH at room temperature (1 h) to yield nano-sized Cu(II)@UiO-

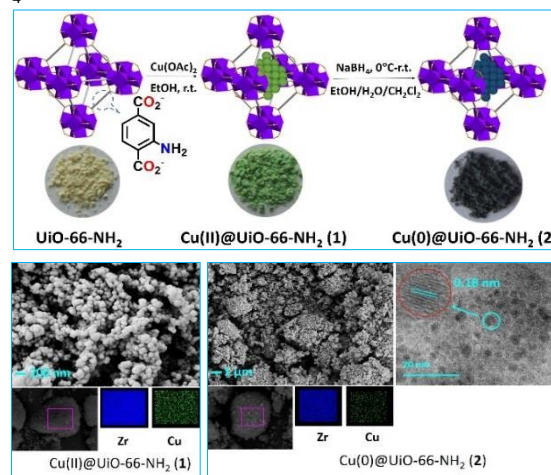NPs- embedded **2** was synthesized by the reduction of **1** with NaBH₄

Fig. 1 Top: synthesis of **1** and **2**. Photographs of the samples are inserted. Bottom: SEM images and SEM-EDS elemental mapping of Cu(II)@UiO-66-NH₂ (**1**) and Cu(0)@UiO-66-NH₂ (**2**), and HR-TEM image of **2**.
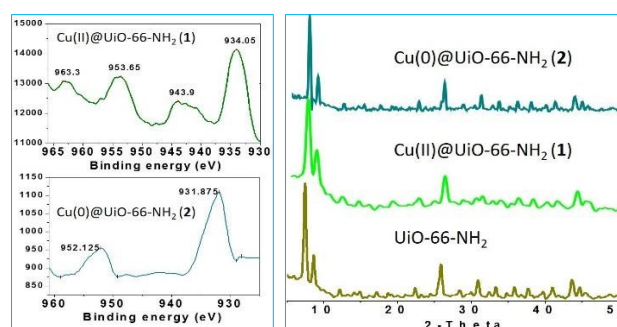
Fig. 2 Left: XPS spectra of Cu(II)@UiO-66-NH₂ (**1**) and Cu(0)@UiO-66-NH₂ (**2**). Right: XRPD patterns of UiO-66-NH₂, Cu(II)@UiO-66-NH₂ (**1**) and Cu(0)@UiO-66-NH₂ (**2**).

in the EtOH/H₂O/CH₂Cl₂ suspended solution along with a distinct colour change (from light green to dark cyan, Scheme 1, ESI). Scanning Electronic Microscopy (SEM) measurement shows that the octahedral particle sizes of **1** and **2** are less than 200 nm and the energy-dispersive X-ray spectra (EDS) indicated that the dispersion of copper species in both **1** and **2** is uniformly

66-NH₂ (**1**) as light green crystalline solid (Scheme 1). The Cu(0)

(Fig. 1). The existence of copper NPs was also confirmed by the high resolution transmission electron microscopy (HR-TEM). As shown in Fig. 1, the spherical shaped copper particles are uniformly distributed in **2** with the average size of ca. 4-6 nm. The atomic lattice fringe with spacing of 0.18 nm corresponding to zero-valent Cu (220) plane was clearly observed.[4]

The oxidation state of the Zr (ESI, Fig. S1) and loaded Cu species before and after reduction was further determined by X-ray photoelectron spectroscopy (XPS). As shown in Fig. 2, the Cu $2p_{3/2}$ and Cu $2p_{1/2}$ peaks at 934.0 eV and 953.7eV, together with the $2p \rightarrow 3d$ satellite peaks between 942.0 and 944.0 eV evidenced that the copper oxidation state in **1** is bivalent.[5] On the other hand, the lower BE peak at 932 eV indicated that the existence of Cu(0) species in **2**.[5] Figure 2 shows that the XRPD patterns of **1** and **2** are in good agreement with that of pristine UiO-66-NH$_2$,[6] demonstrating that the crystallinity and structural integrity of the UiO-66-MOF is well maintained during the copper loading and reducing processes.

The uploaded copper amount in **1** or **2** was determined by inductively coupled plasma (ICP) measurement (ESI Tables S1-S2). The Zr/Cu ratios in **1** and **2** are 1 : 0.2 and 1 : 0.17, respectively. So the corresponding formula of **1** and **2** can be described as 1.2Cu(II)@UiO-66-NH$_2$ and 1.0Cu(0)@UiO-66-NH$_2$, respectively. The Cu-loading of the UiO-66 crystals without amino group was also examined under the same conditions. Notably, the Zr/Cu ratio, however, is only 1 : 0.06 (determined by ICP, ESI, Table S3), indicating that the electron-donating amino group did play an important role in binding and stabilizing Cu species in UiO-66-NH$_2$ crystal matrix.
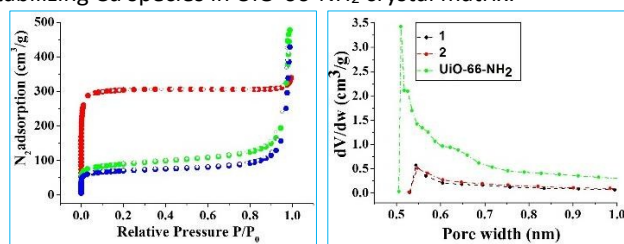

Fig. 3 Left: N$_2$ sorption isotherms at 77K (UiO-66-NH$_2$ (red line), **1** (green line), **2** (blue line); solid symbols: adsorption, open symbols: desorption). Right: the pore widths of UiO-66-NH$_2$, **1** and **2** are centred at 7.6, 6.4 and 6.5 Å, respectively.

The porosities **1** and **2** were demonstrated by the surface area analysis. The N$_2$ sorption measurements (77 K) indicated that the porosities of **1** and **2** are maintained after copper species loading. The lack of hysteresis indicates that the adsorption and desorption mechanisms are similar and that the adsorption is reversible. The Brunauer-Emmett-Teller (BET) surface areas of **1** and **2** determined from N$_2$ adsorption at 77 K were found to be 305.5 m^{2}g^{-1} and 238.8 m^{2}g^{-1}, respectively. Compared to UiO-66-NH$_2$ (1014.6 m^{2}g^{-1}), the surface area decrease clearly resulted from the loaded cooper species. The pore-size distributions of the UiO-66-NH$_2$, **1** and **2** were calculated by nonlocal density functional theory (NLDFT). The UiO-66-NH$_2$, **1** and **2** show narrow pore widths which are centered at 7.6, 6.4 and 6.5 Å, respectively.

Based on above observation, we explored the catalytic activity of the porous copper loaded **1** and **2** for cyclohexene oxidation and styrene reduction, respectively. For cyclohexene oxidation,

the major problem is the selectivity. As reported before, the cyclohexene oxidation is very complicated and could lead to a series of oxidized products, including cyclohexyl hydroperoxide, 2-cyclohexen-1-ol, 2-cyclohexen-1-one, cyclohexene oxide, cyclohexanol, cyclohexanone and 1, 2-cyclohexanediol.[7] In addition, selectivity of the reported cyclohexene oxidation by MOF-catalysts is mainly toward t-butyl-2-cyclohexenyl-1-peroxide instead of α, β-unsaturated ketones or alcohols which are important value-added fine chemicals.[8]

Table 1. Cyclohexene oxidation catalysed by **1**.

entry	T (h)	conv. (%)[a]	select. (%)			TOF [h^{-1}][b]
			(a)	(b)	(c)	
1	12	97	57	43	-	4.1
2	12	96	57	43	-	4.0
3	12	93	55	45	< 0.5	3.9

[a] Determined by GC-MS. [b] TOF = % conversion (mmol of substrate/mmol of cat. h)

The cyclohexene oxidation was carried out in the presence of **1** under solvent-free conditions (Table 1). When a mixture of cyclohexene (1.0 mmol), TBHP (2.0 mmol) and **1** (0.02 mmol, 2% mol Cu) was heated at 80°C for 12h (monitored by GC) to provide the cyclohexen-1-one (55 - 57 %) and 2-cyclohexen-1-ol (43 - 45 %) as the major products (Table 1). Only very tiny amount of cyclohexyl peroxide (< 0.5 %, ESI, Fig. S2) was detected in the third catalytic run. Compared with the most previous examples, **1** herein showed a better catalytic activity (conversion up to 97 %, only slightly lower than that of catalysed by CZJ-1 with PhIO as the oxidant,[9] Table S4). As for chemoselectivity, the oxidation conversion herein is mainly towards cyclohexen-1-one and 2-cyclohexen-1-ol, which is more selective than the most MOFs-catalysed cyclohexene oxidation processes. In those cases, three or more oxidation products were often obtained (ESI, Table S4).

1 herein exhibits a typical heterogeneous catalytic behaviour and it can be easily recovered by centrifugation and directly reused for next catalytic run under the same reaction conditions. As shown in Table 1, no significant decrease in either conversion or selectivity was observed after three runs (ESI, Fig. S3). The XRPD patterns, SEM-EDS and XPS measurements of **1** after three catalytic cycles indicated that the MOF structural integrity, copper valence and dispersion in MOF matrix were well preserved (ESI, Fig. S4), indicating the MOF framework herein is an ideal support for uploading copper species.

In order to further gain insight into the heterogeneous nature of **1**, the hot leaching test was carried out. No further reaction took place without **1** after triggering of the oxidation reaction at 7 h (Fig. S5). This finding demonstrated that **1** exhibits a typical heterogeneous catalyst nature (ESI, Fig. S5). The copper leaching is only 3.0 % after three runs (ESI, Table S5). It is noteworthy that only tiny amount of products b and c were detected when the reaction was carried out using UiO-66-NH$_2$

as catalyst, indicating the catalytic activity is ascribed to the loaded Cu(II) (ESI, Fig. S6).

Besides oxidation, olefin reduction by **2** was also tested. As reported before, high efficient styrene reduction based on metal@MOF-type composite catalysts are mostly focused on precious metal loaded MOFs, such as Pd or Ir-loaded MOF catalysts (Table 2). In contrast, MOF-catalysts without embedded metal species usually show lower catalytic activity (Table 2). On the other hand, the hydrogen source used for hydrogenation is hydrogen gas, sometimes with high pressure. For saving the noble metal natural source and avoiding flammable gases in the reducing process, the cheaper and eco-friendly base metal loaded MOF catalysts and safe hydrogen source are required. In our case, **2** and hydrazine were used as

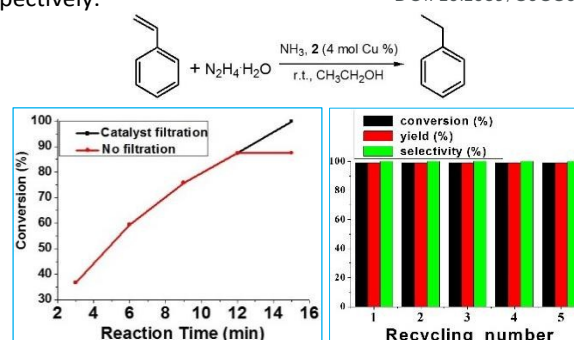catalyst and hydrogen source for styrene hydrogenation, respectively.

Fig. 4 Left: reaction time examination (black line) and leaching test (red line) for styrene hydrogenation catalysed by **2**. Right: recycling catalytic test.

Table 2. Summary of the reported styrene reduction reactions catalysed by the MOF-type heterogeneous catalysts

catalyst	solvent	conditions	yield (%)	TOF[a]	ref.
Pd@MOF-5	styrene	35°C/10 h/ H_2 (1 atm)	100	102.3	10
Pd@MIL-101	styrene	35°C/7 h/ H_2 (1 atm)	100	146.1	11
[Ca(hfipbb)(H$_2$hfipbb)$_{0.5}$(H$_2$O)]·0.7C$_3$H$_6$O	toluene	101°C/2 h/ H_2 (5 atm)	100	254	12
Ni@MesMOF-1	MeOH	r.t./4 h	99	6.5	13
Pd@Tm-MOF	styrene	35°C/1.5 h/ H_2 (1 atm)	10.3	703	14
Pd/ZIF-8	styrene	35°C/1.5 h/ H_2 (1 atm)	4.5	307	
Pd@[Zn$_{17}$thb$_{14}$(₄O)$_4$(H$_2$O)(Me$_2$NH$_2$)]·Me$_2$NH$_2$	styrene	60°C/7 h/ H_2 (1 atm)	100	146.1	15
UiO66–NH$_2$–[LIr]	EtOH	60°C/0.5 h/ H_2 (6 bar)	100	935	16
sal-M-MOF, M = Fe, Co	THF	23°C/18-24 h/ H_2 (40 atm)	100	555.6	17
Pd@UiO-67	THF	r.t./1 h/ H_2 (1 atm)	100	100	18
Pd@[Me$_2$NH$_2$]$_{24}$[Tb$_{12}$(TATB)$_{16}$(HCOO)$_{12}$]	THF	r.t./7 h/ H_2 (1 atm)	100	47.6	18
Pd@Ag-in-UiO-67	THF	r.t./1.6 h/ H_2 (1 atm)	~90.5	54.3	20
Pd-mSiO$_2$@ZIF-8	ethyl acetate	35°C/1 h/ H_2 (1 atm)	100	230.9	21
bpy-MOF-Co	THF	23°C/20 h/ H_2 (40 bar)	100	50	
bpyv-MOF-Co	THF	23°C/20 h/ H_2 (40 bar)	100	50	22
mBPP-MOF-Co	THF	23°C/30 h/ H_2 (40 bar)	100	3333.3	
NacNac-MOF-Co(H)	THF	r.t./1.5 days/ H_2 (40 bar)	100	19444	23
Al$_2$(BDC)$_3$	MeCN	25°C/24 h/ N_2H_4·H_2O	97	0.07	
Fe(BTC)	MeCN	25°C/24 h/ N_2H_4·H_2O	51.5	0.03	
Cu$_3$(BTC)$_2$	MeCN	25°C/24 h/ N_2H_4·H_2O	59.4	0.04	24
Zn-MOF	MeCN	25°C/24 h/ N_2H_4·H_2O	13.9	0.05	
HKUST-1	MeCN	r.t./24 h/N_2H_4·H_2O	16	1.1	
MIL-100 (Fe)	MeCN	r.t./24 h/N_2H_4·H_2O	44	0.29	25
MIL-53 (Al)	MeCN	r.t./24 h/N_2H_4·H_2O	38	0.74	
2	EtOH	r.t./15 min/N_2H_4·H_2O	100	100	**This work**

[a]TOF = calculated at initial reaction rate as moles of product formed per hour and per mole of catalyst or given in the corresponding paper.

In the typical procedure, styrene (0.14 mmol, 16 μL) was treated with N_2H_4·H_2O (80 wt %, 20 μL) and NH_3·H_2O (18 wt %, 10 μL) in the presence of **2** (10 mg, 4 mol % Cu) under ambient temperature. The reaction was monitored by GC. As shown in Fig. 4, the catalytic activity of **2** in styrene hydrogenation is highly active, and the styrene hydrogenation was clean and proceeded very fast (ca. 15 min.) under ambient temperature, with > 99 % conversion and 100 % selectivity (ESI, Table S6, Fig. S7). To our knowledge, this might be the fastest MOF catalyst-assisted styrene hydrogenation to date.

It is similar to **1**, **2** also exhibits typical heterogeneous catalyst nature in styrene hydrogenation and can be readily recovered
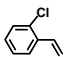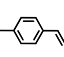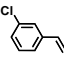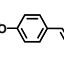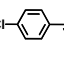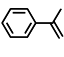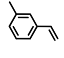
and reused for five times without decrease in conversion and selectivity (Fig. 4). The Cu leaching after five catalytic runs was determined to be ca. 5.8 % (ESI, Table S7). After the fifth cycle, the crystallinity and MOF structural integrity of the recovered **2** was confirmed by XRPD (ESI, Fig. S8). HR-TEM analysis revealed that the mean diameter of the Cu(0) NPs slightly increases after five runs, which might be caused the slight agg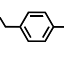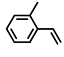regation of Cu NPs (ESI, Fig. S8). SEM-EDS measurement shows that the morphology and high copper dispersion were still maintained even after five catalytic runs (ESI, Fig. S9). The XPS spectrum confirmed that no copper valent change occurred after catalysis, indicating Cu(0) species can be well

COMMUNICATION

Journal Name

stabilized in the MOF matrix during the catalytic process under the reaction conditions (ESI, Fig. S9). In addition, no further hydrogenation occurred after removal of **2** from the reaction system (Fig. 4).

For confirmation of the encapsulated Cu(0) NPs being responsible for the catalytic activity, a series of control experiments were performed. When the reaction was carried out using Cu(OAc)$_2$, UiO-66-NH$_2$ or **1** as the catalyst under the same reaction conditions, the corresponding yields for ethylbenzene are 59, 18 and 57 %, respectively. Only 9 % of ethylbenzene was obtained when styrene hydrogenation was performed without any catalyst (ESI, Fig. S10). So the loaded Cu(0) NPs in UiO-66-MOF matrix is responsible for the catalytic activity.

Table 3. Hydrogenation reactions of the vinylbenzenes with different substituted groups catalysed by **2**.

entry	substrate	yield^a	entry	substrate	yield^a
1		98 %	6		98 %
2		97 %	7		85 %
3		94 %	8		63 %
4		96 %	9		50 %
5		94 %			

^{a} Determined by GC.

After that, we investigated the catalytic activity of **2** for hydrogenation of a series of other substituted vinyl benzenes (Table 3). We found that **2** exhibits high reactivity with excellent conversions toward nine-atom mono-substituted vinyl benzenes (entries 1-6, yields, 94-98 %) regardless of the electron-donating or electron-withdrawing groups and positions of the substituents. On the other hand, the hydrogenating yields for ten-atom substrates (entries 7 and 8, yields, 63-85 %) or 1.1-disubstituted styrene (entry 9, yield, 50 %) are low, which might be explained by the stereo-hindrance effect.

In conclusion, two base metal loaded MOF catalysts Cu(II)@UiO-66-NH$_2$ (**1**) and Cu(0)@UiO-66-NH$_2$ (**2**) have been obtained and studied. The main feature of these new materials is their high catalytic activity for olefin oxidation and hydrogenation under mild conditions. This makes them the real candidates to provide an alternative to conventional noble metal-based corresponding catalysts.
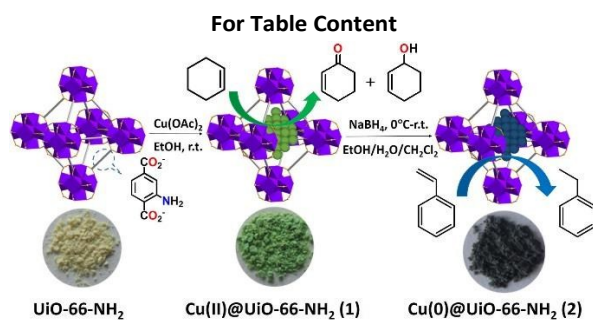
Notes and references

1 (a) A. Corma, H. García and F. X. Llabrés i Xamena, *Chem. Rev.*, 2010, **110**, 4606–4655. (b) M. Yoon, R. Srirambalaji, K. Kim, *Chem. Rev.*, 2012, **112**, 1196–1231. (c) A. H. Chughtai, N. Ahmad, H. A. Younus, A. Laypkov, F. Verpoort, *Chem. Soc. Rev.*, 2015, **44**, 6804-6849.
2 (a) A. Dhakshinamoorthy, H. Garcia, *Chem. Soc. Rev.*, 2012, **41**, 5262-5284. (b) H. R. Moon, D.-W. Lim, M, P. Suh, *Chem. Soc. Rev.*, 2013, **42**, 1807-1824.
3 N. C. Thacker, Z. Lin, T. Zhang, J. C. Gilhula, C. W. Abney, W. Lin, *J. Am. Chem. Soc.*, 2016, **138**, 3501-3509.
4 A. D. Brumbaugh, K. A. Cohen, S. K. St. Angelo, *Sustainable Chem. Eng.*, 2014, **2**, 1933–1939.
5 (a) J. Gong, H. Yue, Y. Zhao, S. Zhao, L. Zhao, J. Lv, S. Wang, X. Ma, *J. Am. Chem. Soc.*, 2012, **134**, 13922–13925. (b) P. Liu, E. J. M. Hensen, *J. Am. Chem. Soc.*, 2013, **135**, 14032–14035.
6 S. J. Garibay, S. M. Cohen, *Chem. Commun.*, 2010, **46**, 7700-7702.
7 (a) D. Sun, F. Sun, X. Deng, Z. Li, *Inorg. Chem.*, 2015, **54**, 8639−8643. (b) A. Alfayate, C. Márquez-Álvarez, M. Grande-Casas, M. Sánchez-Sánchez, J. Pérez-Pariente, *Catalysis Today*, 2014, **227**, 57–64. (c) Y. Cao, H. Yu, F. Peng, H. Wang, *ACS Catal.*, 2014, **4**, 1617−1625. (d) M. Sanchez-Sanchez, I. de Asua, D. Ruano, K. Diaz, *Cryst. Growth Des.*, 2015, **15**, 4498−4506.
8 (a) K. J. Gagnon, C. M. Beavers, A. Clearfield, *J. Am. Chem. Soc.*, 2013, **135**, 1252-1255. (b) H.-Y. Ren, R.-X. Yao, X.-M. Zhang, *Inorg. Chem.*, 2015, **54**, 6312–6318.
9 M.-H. Xie, X.-L. Yang, Y. He, J. Zhang, B. Chen, C.-D. Wu, *Chem. Eur. J.*, 2013, **19**, 14316 – 14321.
10 M. Sabo, A. Henschel, H. Frode, E. Klemm, S. Kaskel, *J. Mater. Chem.*, 2007, **17**, 3827–3832.
11 A. Henschel, K. Gedrich, R. Kraehnert, S. Kaskel, *Chem. Commun.*, **2008**, 4192–4194.
12 A. E. P. Prats, V. A. de la PeÇa-O'Shea, M. Iglesias, N. S. ngeles Monge, E. Gutirrez-Puebla, *ChemCatChem*, 2010, **2**, 147-149.
13 Y. K. Park, S. B. Choi, H. J. Nam, D.-Y. Jung, H. C. Ahn, K. Choi, H. Furukawa, J. Kim, *Chem. Commun.*, 2010, **46**, 3086–3088.
14 Y. Pan, D. Ma, H. Liu, H. Wu, D. He, Y. Li, *J. Mater. Chem.*, 2012, **22**, 10834-10839.
15 Y.-X. Tan, Y.-P. He, J. Zhang, *Chem. Commun.*, 2014, **50**, 6153-6156.
16 A. M. Rasero-Almansa, A. Corma, M. Iglesias, F. Sánchez, *Green Chem.*, 2014, **16**, 3522–3527.
17 K. Manna, T. Zhang, M. l. Carboni, C. W. Abney, W. Lin, *J. Am. Chem. Soc.*, 2014, **136**, 13182−13185.
18 L. Chen, X. Chen, H. Liu, C. Bai, Y. Li, *J. Mater. Chem. A*, 2015, **3**, 15259–15264.
19 Y.-H. Han, C.-B. Tian, P. Lin, S.-W. Du, *J. Mater. Chem. A*, 2015, **3**, 24525–24531.
20 L. Chen, B. Huang, X. Qiu, X. Wang, R. Luque, Y. Li, *Chem. Sci.*, 2016, **7**, 228–233.
21 B. Xi, Y. C. Tan, H. C. Zeng, *Chem. Mater.*, 2016, **28**, 326−336.
22 T. Zhang, K. Manna, W. Lin, *J. Am. Chem. Soc.*, 2016, **138**, 3241–3249.
23 N. C. Thacker, Z. Lin, T. Zhang, J. C. Gilhula, C. W. Abney, W. Lin, *J. Am. Chem. Soc.*, 2016, **138**, 3501–3509.
24 A. Dhakshinamoorthy, M. Alvaro, H. Garcia, *Adv. Synth. Catal.*, 2009, **351**, 2271 − 2276.
25 P. Garca-Garca, M. Muller, A. Corma, *Chem. Sci.*, 2014, **5**, 2979–3007.

For Table Content

UiO-66-NH$_2$ Cu(II)@UiO-66-NH$_2$ (1)   Cu(0)@UiO-66-NH$_2$ (2)

Two copper-loaded MOF materials Cu(II)@Ui-O-66-NH$_2$ (**1**) and Cu(0)@UiO-66-NH$_2$ (**2**), which can be highly active heterogeneous catalysts for olefin oxidation and hydrogenation, are reported.